

Two-dimensional molecular-based ferrimagnets incorporating decamethylmetallocenium cations

Yu Pei,^{a†} Scott S. Turner,^{b,c} Léopold Fournes,^b Joel S. Miller^{a*} and Olivier Kahn^{b,c}

^aDepartment of Chemistry, University of Utah, Salt Lake City, UT 84112, USA

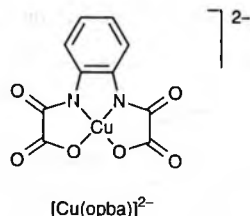
^bInstitut de Chimie de la Matière Condensée de Bordeaux, UPR CNRS no. 9048, 33608 Pessac, France

^cLaboratoire des Sciences Moléculaires, Institut de Chimie de la Matière Condensée de Bordeaux, UPR CNRS no. 9048, 33608 Pessac, France

Four new molecular-based magnets have been synthesized, and their magnetic properties have been investigated in detail. Their formulae are $[M'(C_5Me_5)_2]_2M_2[Cu(opba)]_3 \cdot (DMSO)_x(H_2O)_y$ with $M' = Fe$, $M = Mn$, $x = 5$, $y = 4$ (**1**), $M' = Fe$, $M = Co$, $x = 6$, $y = 4$ (**2**), $M' = Co$, $M = Mn$, $x = 5.5$, $y = 4$ (**3**) and $M' = Co$, $M = Co$, $x = 5.5$, $y = 4$ (**4**) [$opba = ortho$ -phenylenebis(oxamato)]. The decamethylmetallocenium cations $[Fe(C_5Me_5)_2]^+$ and $[Co(C_5Me_5)_2]^+$ are most probably located between the anionic honeycomb-like networks $Mn_2[Cu(opba)]_3$ and $Co_2[Cu(opba)]_3$. Compounds **1–4** are two-dimensional ferrimagnets exhibiting a spontaneous magnetization below a critical temperature, T_c , of 14 K for **1**, 27 K for **2**, 13 K for **3** and 27.5 K for **4**. Compounds **1** and **3**, with Mn^{II} ions in the layered framework structure, do not exhibit magnetic hysteresis, while **2** and **4**, with Co^{II} in the layered framework structure, exhibit a wide magnetic hysteresis loop. The coercive fields at 2 K are found to be equal to 3.5×10^3 Oe for **2** and 5.3×10^3 Oe for **4**. The latter is one of the largest values reported so far for a molecular-based magnet. The Mössbauer spectra for **1** and **2** have been recorded at various temperatures. These spectra suggest that the $[Fe(C_5Me_5)_2]^+$ units occupy two sites between the layers with a 50/50 distribution, and that they are not directly involved in the long-range magnetic ordering.

$[Fe(C_5Me_5)_2][TCNE]$ $\{[Fe(C_5Me_5)_2]^+ = \text{decamethylferrocenium cation}, [TCNE]^- = \text{tetracyanoethene anion}\}$, and $MnCu(pbaOH)(H_2O)_3$ [$pbaOH = 2$ -hydroxy-1,3-propylenebis(oxamato)] are prototype molecular-based magnets with linear chain structures.^{1,2} For the former, the interaction between adjacent $[Fe(C_5Me_5)_2]^+$ and $[TCNE]^-$ spin-bearing units along the chain is ferromagnetic, and the ferromagnetic chains couple ferromagnetically within the lattice, which leads to a three-dimensional ferromagnetic ordering at $T_c = 4.8$ K.³ For the latter compound, the adjacent Mn^{II} and Cu^{II} ions couple antiferromagnetically along the chain, affording ferrimagnetic chains, and these chains couple ferromagnetically within the lattice, which leads to a long-range magnetic ordering at $T_c = 4.6$ K.⁴ By partial dehydration, this critical temperature can be increased up to 30 K.⁵ Since 1986, several additional metallocenium electron-transfer salts with ferromagnetic states at low temperatures have been characterized.^{6–11} Similarly, other $Mn^{II}Cu^{II}$ molecular compounds exhibiting a spontaneous magnetization below a certain critical temperature have been described;¹² some of these have a chain structure^{13,14} while others have a layered structure.¹⁵ One such compound has a three-dimensional structure resulting from the unprecedented interlocking of two perpendicular honeycomb-like networks.^{16,17}

To date, metallocenium-containing and bimetallic compounds have corresponded to two facets of the area of molecular-based magnets.^{18,19} In this paper, we explore the possibility of combining the two classes of compounds. The general formula of the layered bimetallic magnets mentioned above is $cat_2M_2[Cu(opba)]_3 \cdot S$ [$cat^+ = \text{a monovalent cation}$, $S = \text{solvent molecules}$; $opba = ortho$ -phenylenebis(oxamato); $opba$ may be replaced by $pba = 1,3$ -propylenebis(oxamato)].



M may be either Mn^{II} or Co^{II} . Till now, compounds in which cat^+ is either an alkaline or an organic cation have been prepared.¹² In addition, a magnet in which the counter-anion is divalent, of formula $[Ru(bipy)_3]Mn_2[Cu(opba)]_3 \cdot 13H_2O$, has been described.²⁰ Herein, we focus on the layered compounds for which cat^+ is either decamethylferrocenium with a spin-doublet ground state, or decamethylcobaltocenium with a closed-shell ground state. More precisely, we report on the synthesis and the magnetic properties of four compounds $[M'(C_5Me_5)_2]_2M_2[Cu(opba)]_3 \cdot (DMSO)_x(H_2O)_y$ with $M' = Fe$, $M = Mn$, $x = 5$, $y = 4$ (**1**), $M' = Fe$, $M = Co$, $x = 6$, $y = 4$ (**2**), $M' = Co$, $M = Mn$, $x = 5.5$, $y = 4$ (**3**) and $M' = Co$, $M = Co$, $x = 5.5$, $y = 4$ (**4**). These compounds will be abbreviated hereafter as $M'_2M_2Cu_3$. We also report on the Mössbauer investigation of **1** and **2**.

Experimental

Syntheses

$[Fe(C_5Me_5)_2](BF_4)$ was synthesized as described previously,³ and $[Co(C_5Me_5)_2](PF_6)$ was purchased from Strem. All the chemicals used were of reagent grade. $[Fe(C_5Me_5)_2]Mn_2[Cu(opba)]_3 \cdot (DMSO)_5(H_2O)_4$ **1** was synthesized as follows: 103 mg (0.25 mmol) of $Na_2[Cu(opba)]_3 \cdot 3H_2O$ ¹⁵ and 207 mg (0.50 mmol) of $[Fe(C_5Me_5)_2](BF_4)_2$ were dissolved in 20 ml of a 4:1 DMSO–acetone mixture. After heating the resulting green solution to ca. 50 °C, 31 mg (0.125 mmol) of $Mn(CH_3CO_2)_2 \cdot 4H_2O$ was added with stirring. After stirring for 10 min the mixture was allowed to cool to room temperature. The precipitate was filtered off, washed with the DMSO–acetone mixture, and dried under vacuum, affording 100 mg of the green–blue product (yield with respect to $[Cu(opba)]^{2-}$ and $[Fe(C_5Me_5)_2]^+$, 19%). Elemental analysis for $C_{70}H_{72}N_6O_{18}Fe_2Mn_2Cu_3 \cdot 5DMSO \cdot 4H_2O$: found (calc.) C, 44.36 (44.5); H, 4.86 (5.1); N, 3.89 (3.9); S, 7.81 (7.4); Fe, 5.09 (5.2); Mn, 5.79 (5.1); Cu, 8.59 (8.8).

$[Fe(C_5Me_5)_2]Co_2[Cu(opba)]_3 \cdot (DMSO)_6(H_2O)_4$ **2** was prepared in the same way as **1**, using 31 mg of $Co(CH_3CO_2)_2 \cdot 4H_2O$. A blue–grey product was obtained (130 mg; yield, 23%). Elemental analysis for $C_{70}H_{72}N_6O_{18}Fe_2Co_2Cu_3 \cdot 6DMSO \cdot 4H_2O$: found (calc.) C, 43.64

† Permanent address: Laboratoire de Chimie Inorganique, Université de Paris Sud, 91405 Orsay, France.

(43.8); H, 4.65 (5.2); N, 3.98 (3.7); S, 8.56 (8.6); Fe, 4.91 (5.0); Co, 5.51 (5.25); Cu, 8.52 (8.5).

$[\text{Co}(\text{C}_5\text{Me}_5)_2]_2\text{Mn}_2[\text{Cu}(\text{opba})]_3 \cdot (\text{DMSO})_{5.5}(\text{H}_2\text{O})_4$ **3** was prepared from 237 mg (0.5 mmol) of $[\text{Co}(\text{C}_5\text{Me}_5)_2](\text{PF}_6)$ and 103 mg (0.25 mmol) of $\text{Na}_2[\text{Cu}(\text{opba})] \cdot 3\text{H}_2\text{O}$ dissolved in 10 ml of DMSO. The resulting solution was heated to ca. 50 °C, then 36 mg (0.147 mmol) of $\text{Mn}(\text{CH}_3\text{CO}_2)_2 \cdot 4\text{H}_2\text{O}$ was added with stirring. The mixture was allowed to cool to room temperature and to stand overnight. The precipitate was filtered off, washed with DMSO and dried under vacuum, yielding 80 mg of a green product (yield, 14%). Elemental analysis for $\text{C}_{70}\text{H}_{72}\text{N}_6\text{O}_{18}\text{Co}_2\text{Mn}_2\text{Cu}_3 \cdot 5.5\text{DMSO} \cdot 4\text{H}_2\text{O}$: found (calc.) C, 44.15 (44.1); H, 4.90 (5.2); N, 3.72 (3.8); S, 7.91 (8.0); Co, 5.00 (5.3); Mn, 4.86 (5.0); Cu, 8.53 (8.6).

$[\text{Co}(\text{C}_5\text{Me}_5)_2]_2\text{Co}_2[\text{Cu}(\text{opba})]_3 \cdot (\text{DMSO})_{5.5}(\text{H}_2\text{O})_4$ **4** was prepared in the same way as **3**, using cobalt(II) acetate instead of manganese(II) acetate. Compound **4** was obtained as a green-grey product (100 mg; yield, 18%). Elemental analysis for $\text{C}_{70}\text{H}_{72}\text{N}_6\text{O}_{18}\text{Co}_4\text{Cu}_3 \cdot 5.5\text{DMSO} \cdot 4\text{H}_2\text{O}$: found (calc.) C, 44.05 (43.95); H, 5.08 (5.15); N, 3.75 (3.8); S, 7.58 (8.0); Co, 10.12 (10.65); Cu 8.34 (8.6).

Magnetic measurements

These were carried out with a Quantum Design MPMS-5S SQUID magnetometer, working in both dc and ac modes between 2 and 300 K, and from 0 to 5 T. The ac measurements were made at a field oscillation frequency of 125 Hz and a drive amplitude of 1 Oe.

Mössbauer spectra

These were recorded with a constant acceleration HALDER-type spectrometer, using a room-temperature ^{57}Co (Rh matrix) source in transmission geometry, equipped with a variable-temperature cryostat. The isomer shifts were determined with respect to metallic iron at room temperature.

Results

Magnetic properties

The dependences of both the dc and ac magnetic susceptibilities, and the field dependence of the magnetization for **1–4** were studied.

Temperature dependence of the dc magnetic susceptibility. The $\chi_{\text{M}}T$ vs. T plots for compounds **1–4** exhibit the same general behaviour (χ_{M} is the molar magnetic susceptibility measured at a field of 10^3 Oe; T is the temperature). The curve for $\text{Fe}_2\text{Mn}_2\text{Cu}_3$ **1** is shown in Fig. 1. For this compound, at room temperature $\chi_{\text{M}}T$ is $9.77 \text{ cm}^3 \text{ K mol}^{-1}$, which is slightly lower than expected for two low-spin Fe^{III} , two high-spin Mn^{II} and three Cu^{II} isolated ions (expected value ca. $12 \text{ cm}^3 \text{ K mol}^{-1}$). As T is lowered, $\chi_{\text{M}}T$ decreases slowly and exhibits a rounded minimum at 132 K with $\chi_{\text{M}}T = 9.18 \text{ cm}^3 \text{ K mol}^{-1}$, and then it increases very rapidly to a maximum of $332 \text{ cm}^3 \text{ K mol}^{-1}$ at 14 K. This behaviour is characteristic of a ferrimag-

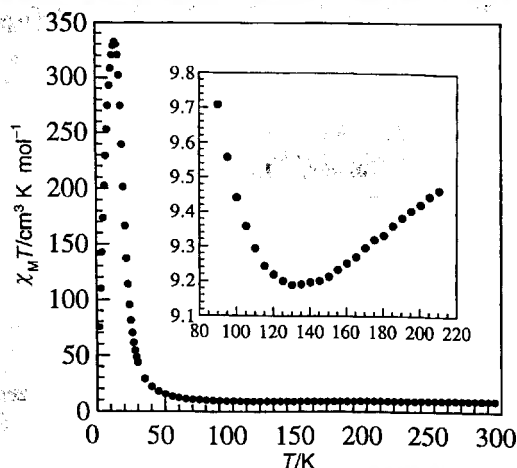


Fig. 1 $\chi_{\text{M}}T$ vs. T plot for $\text{Fe}_2\text{Mn}_2\text{Cu}_3$ **1**, measured with an external field of 10^3 Oe. The insert emphasizes the characteristic minimum of $\chi_{\text{M}}T$ around 132 K.

netic material.¹⁸ At high temperature, $\chi_{\text{M}}T$ approaches the paramagnetic limit. As T is lowered, the decrease in $\chi_{\text{M}}T$ corresponds to a short-range order where the local spins S_{Cu} and S_{Mn} of adjacent metal ions are aligned antiparallel but have no correlation with neighbouring MnCu units. As T is lowered further, below the $\chi_{\text{M}}T$ minimum, the randomizing thermal effects are reduced and the correlation length increases. This leads to a spontaneous magnetization below a critical temperature, T_{C} . A maximum of $\chi_{\text{M}}T$ occurs owing to the effects of an induced demagnetizing field, and its position is highly field-dependent. Table 1 gives the values of $\chi_{\text{M}}T$ at 300 K together with the temperature of the minimum of $\chi_{\text{M}}T$ and the value of this minimum. In each case, the $\chi_{\text{M}}T$ value at 300 K is lower than expected for the paramagnetic limit, which indicates that the antiferromagnetic interaction is already operative. The compounds have decreasing room-temperature $\chi_{\text{M}}T$ values in the order $\text{Fe}_2\text{Mn}_2\text{Cu}_3$ **1** > $\text{Co}_2\text{Mn}_2\text{Cu}_3$ **3** > $\text{Fe}_2\text{Co}_2\text{Cu}_3$ **2** > $\text{Co}_2\text{Co}_2\text{Cu}_3$ **4**. As expected, those materials containing the $[\text{Fe}(\text{C}_5\text{Me}_5)_2]^+$ cation have larger $\chi_{\text{M}}T$ values than the corresponding compounds containing the $[\text{Co}(\text{C}_5\text{Me}_5)_2]^+$ cation, reflecting the paramagnetic vs. diamagnetic nature of the cations.

Ac susceptibility measurements. Ac magnetic susceptibility measurements can be used to determine accurate values of T_{C} , the temperature below which a substance exhibits spontaneous magnetization, and also to investigate magnetization relaxation processes within a sample.²¹ The ac experiment yields both the in-phase (or 'real') volume susceptibility (χ') vs. temperature, and the out-of-phase (or 'imaginary') signal (χ'') vs. temperature. The out-of-phase component is proportional to the energy absorbed by the substance from the oscillating field, and when relaxation effects become appreciable, this component becomes non-zero. A non-zero imaginary component is therefore indicative of the presence of net magnetic moments when the sample

Table 1 Critical temperatures, T_{C} , deduced from ac magnetic susceptibility measurements, and characteristic values in the $\chi_{\text{M}}T$ vs. T curves and magnetization vs. field curves for compounds **1–4**

compound	T_{C}/K	minimum of $\chi_{\text{M}}T$		hysteresis loop		
		$\chi_{\text{M}}T$ (at 300 K)/ $\text{cm}^3 \text{ K mol}^{-1}$	$\chi_{\text{M}}T$ / $\text{cm}^3 \text{ K mol}^{-1}$	T/K	coercive field/Oe	$M_{\text{s}}/\mu_{\text{B}}$
$\text{Fe}_2\text{Mn}_2\text{Cu}_3$ 1	14	9.77	9.18	132	<20	8.89
$\text{Fe}_2\text{Co}_2\text{Cu}_3$ 2	27	7.39	6.09	95	3.5×10^3	4.22
$\text{Co}_2\text{Mn}_2\text{Cu}_3$ 3	13	8.11	7.55	135	<20	6.6
$\text{Co}_2\text{Co}_2\text{Cu}_3$ 4	27.5	5.79	4.64	95.5	5.3×10^3	2.76

is no longer in the paramagnetic regime. The χ'' vs. T plots for $\text{Co}_2\text{Mn}_2\text{Cu}_3$ **3** and $\text{Co}_2\text{Co}_2\text{Cu}_3$ **4** are shown in Fig. 2. T_C is taken as the point when the correlation length is infinite, i.e. when the sample effectively consists of one domain, and the energy absorbed and χ'' are at a maximum. The T_C values for **1–4** are given in Table 1.

Field dependence of the magnetization. The field dependences of the magnetization, M , for **1–4** were investigated between $\pm 5 \times 10^4$ Oe at 2 K. The plot for $\text{Co}_2\text{Mn}_2\text{Cu}_3$ **3** is shown in Fig. 3, and those for $\text{Fe}_2\text{Co}_2\text{Cu}_3$ **2** and $\text{Co}_2\text{Co}_2\text{Cu}_3$ **4** are compared in Fig. 4. $\text{Co}_2\text{Mn}_2\text{Cu}_3$ **3** does not exhibit a detectable hysteresis effect upon cycling the applied field. Its saturation magnetization value of $6.6 \mu_B$ corresponds well with the expectation for all the S_{Mn} local spins aligned along the field direction and the S_{Cu} local spins aligned in the opposite direction. Approximately 90% of the saturation magnetization is reached within a field of a few hundred Oersted. The plot for $\text{Fe}_2\text{Mn}_2\text{Cu}_3$ **1** is similar to that for $\text{Co}_2\text{Mn}_2\text{Cu}_3$ **3**, except that the saturation magnetization is $8.89 \mu_B$. This corresponds

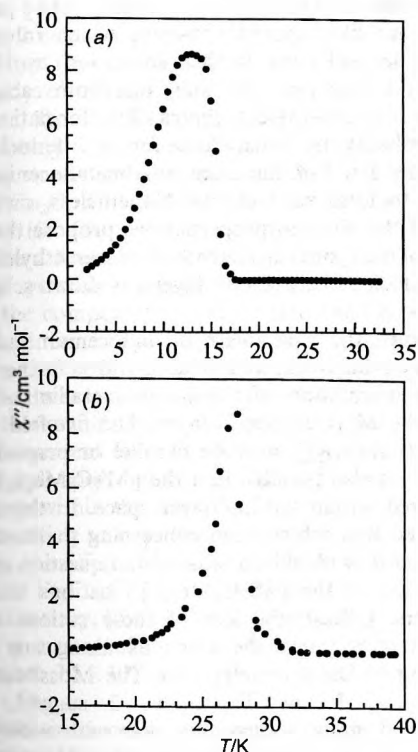


Fig. 2 Ac out-of-phase molar magnetic susceptibility, χ'' , vs. temperature plots for $\text{Co}_2\text{Mn}_2\text{Cu}_3$ **3** (a) and $\text{Co}_2\text{Co}_2\text{Cu}_3$ **4** (b). Measurements were made at 125 Hz with a drive amplitude of 1 Oe.

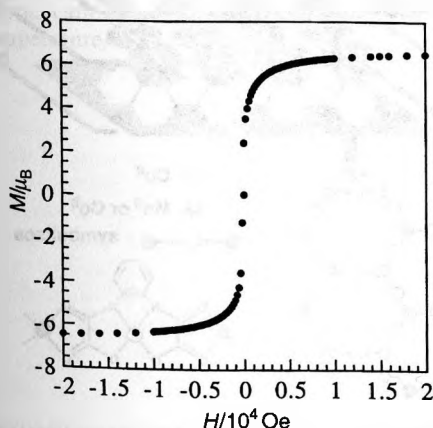


Fig. 3 Magnetization vs. field plot at 2 K for $\text{Co}_2\text{Mn}_2\text{Cu}_3$ **3**

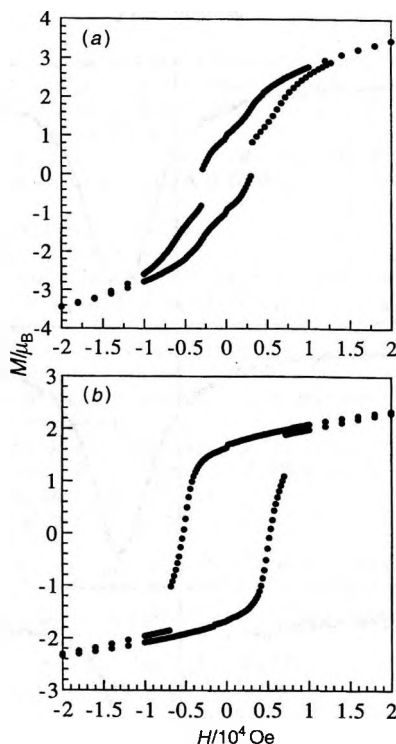


Fig. 4 Magnetization vs. field plots at 2 K for $\text{Fe}_2\text{Co}_2\text{Cu}_3$ **2** (a) and $\text{Co}_2\text{Co}_2\text{Cu}_3$ **4** (b)

to what is expected for S_{Mn} and S_{Fe} local spins (from low-spin Fe^{III}) aligned along the field direction in opposition to the S_{Cu} local spins. In contrast, the saturation magnetization values for $\text{Fe}_2\text{Co}_2\text{Cu}_3$ **2** and $\text{Co}_2\text{Co}_2\text{Cu}_3$ **4** are not achieved at 5 T, and the maximum values attained are 4.22 and $2.76 \mu_B$, respectively. Both **2** and **4** exhibit magnetic hysteresis loops. The coercive fields are as large as 3.5×10^3 Oe for **2** and 5.3×10^3 Oe for **4**. The general shapes of the hysteresis loops are unusual. Both show steps, the sizes of which correspond to approximately $1 \mu_B$ (or $S = 1/2$).

Mössbauer spectra

The two compounds containing the $[\text{Fe}(\text{C}_5\text{Me}_5)_2]^+$ cation, $\text{Fe}_2\text{Mn}_2\text{Cu}_3$ **1** and $\text{Fe}_2\text{Co}_2\text{Cu}_3$ **2**, were investigated by Mössbauer spectroscopy at 293, 17.5 and 4.2 K. The spectra are shown in Fig. 5 for **1** and Fig. 6 for **2**.

At 293 K, the spectra for **1** and **2** are very similar, and are typical of low-spin Fe^{III} ions.^{3,22} In other respects, the recoilless factor is weak, which leads to a rather poor resolution and a broadening of the lines. These features usually reveal that the particle sizes are very small, which is consistent with our failure to grow single crystals suitable for X-ray diffraction. For both **1** and **2**, our attempts to fit the spectra with a single-site model failed. On the other hand, a satisfactory fitting was achieved with a two-site model and a 50/50 distribution. For **1**, the isomer shifts, δ , are found to be $0.35(3) \text{ mm s}^{-1}$ for one of the sites and $0.45(3) \text{ mm s}^{-1}$ for the other; the corresponding mean quadrupole splittings, Δ , are found to be $\langle 0.37 \rangle$ and $\langle 0.32 \rangle \text{ mm s}^{-1}$, respectively. For **2**, $\delta = 0.35(3)$ and $0.45(3) \text{ mm s}^{-1}$; the corresponding Δ values were found to be $\langle 0.35 \rangle$ and $\langle 0.15 \rangle \text{ mm s}^{-1}$, respectively.

The spectra are similar at 17.5 K. However, a broadening of the resonance is observed along with the appearance of satellites. These slight modifications are more pronounced for compound **2**; they are due to the fact that the low-spin Fe^{III} ions begin to see an internal magnetic field, as a consequence of which T_C is 27 K for **2** and 14 K for **1**.

Well below their ordering temperatures, at 4.2 K, **1** and **2** exhibit very different spectra. For **1**, the resonance is broadened

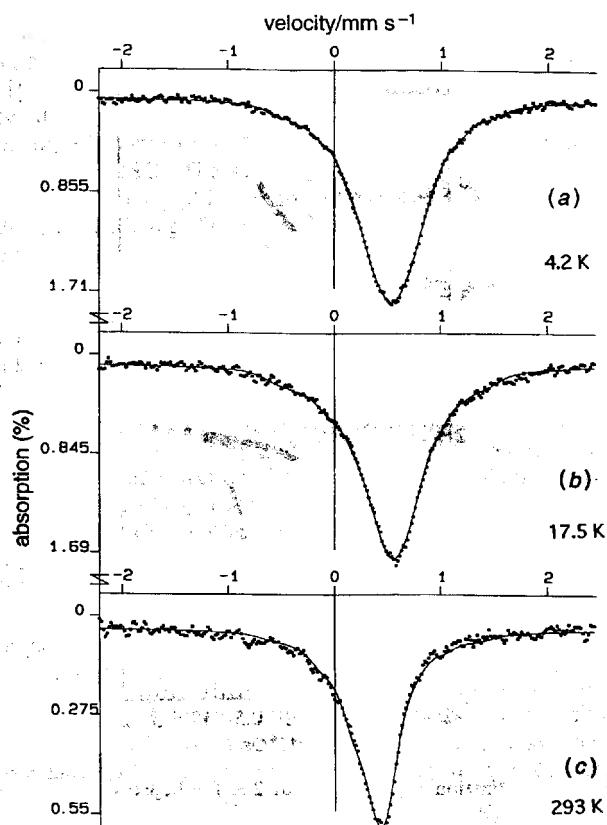


Fig. 5 Mössbauer spectra at 293, 17.5 and 4.2 K for $\text{Fe}_2\text{Mn}_2\text{Cu}_3$ 1

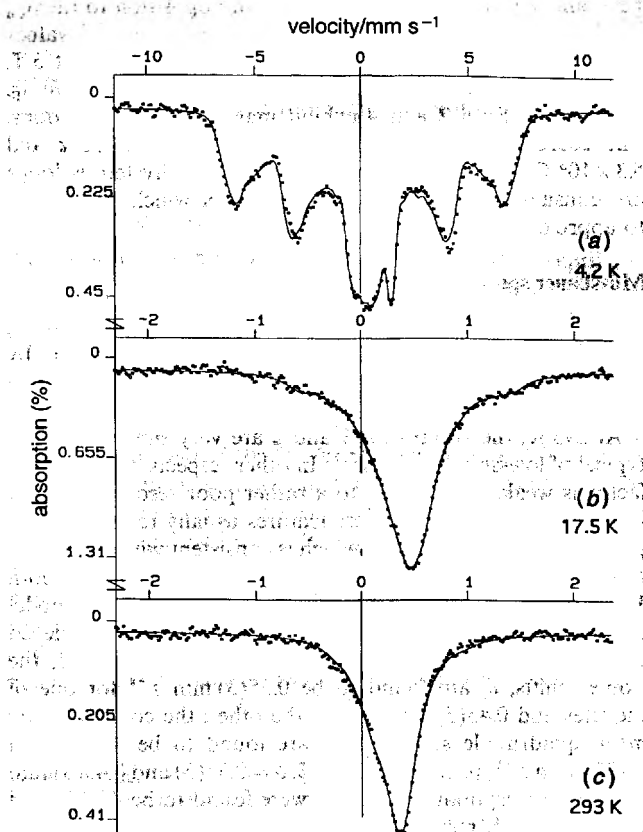


Fig. 6 Mössbauer spectra at 293, 17.5 and 4.2 K for $\text{Fe}_2\text{Co}_2\text{Cu}_3$ 2

further with respect to the situation at 17.5 K, whereas for 2, a six-line Zeeman-split spectrum is observed, characteristic of a decamethylferrocenium ion in a magnetically ordered phase. The spectrum could not be fitted with a single value of the internal field. However, a good simulation of the experimental

spectrum can be obtained with two values of the internal field, 36 and 16 T. This simulation also indicates that a small amount (about 15%) of Fe^{III} ions do not see the internal field.

The information arising from this Mössbauer investigation may be summed up as follows: (i) 1 and 2 crystallize with very small particle sizes; (ii) the decamethylferrocenium cations seem to occupy two sites with an approximately 50/50 distribution. It is then tempting to assign these two sites to the parallel and perpendicular orientations of the C_5Me_5 rings with respect to the layers; (iii) the low-spin Fe^{III} ions of the $[\text{Fe}(\text{C}_5\text{Me}_5)_2]^+$ units begin to feel the internal field arising from the long-range magnetic ordering well below the critical temperatures of 14 K for 1 and 27 K for 2. This crucial information indicates that the $[\text{Fe}(\text{C}_5\text{Me}_5)_2]^+$ units are not directly involved in this long-range magnetic ordering.

Discussion

Although structural information is unavailable for 1–4, the structure of $\text{cat}_2\text{M}_2[\text{Cu}(\text{opba})]_3\cdot\text{S}$ where cat^+ is 2-(4-*N*-methylpyridinium)-4,4,5,5-tetramethylimidazoline-1-oxyl-3-oxide has been determined.^{16,17} This structure consists of two perpendicular honeycomb-like layered networks which interpenetrate. These two networks are further connected by the radical cations that bridge two Cu^{II} ions, one from each network, resulting in Cu – cat – Cu – cat chains. The formation of such chains is probably the driving force for the interlocking of the two networks. For 1–4, the decamethylmetallocenium cations are unable to form such chains. Nonetheless, owing to the similarity of the physical properties, we propose that 1–4 are comprised of hexagonal layers with the decamethylmetallocenium cations located between the layers, as shown schematically in Fig. 7.

Concerning the decamethylmetallocenium derivatives investigated in this work, we are faced with a further question, namely the orientation of the organometallic cations with respect to the $\text{M}_2[\text{Cu}(\text{opba})]_3$ layer. The five-fold symmetry axis of $[\text{M}'(\text{C}_5\text{Me}_5)_2]^+$ may be parallel or perpendicular to the layers. It is also possible that the $[\text{M}'(\text{C}_5\text{Me}_5)_2]^+$ cations are disordered within the interlayer space. In this respect, it may be noted that information concerning the basal spacing in compounds 1–4 would not answer the question concerning the orientation of the $[\text{M}'(\text{C}_5\text{Me}_5)_2]^+$ cations with respect to the layers. Indeed, the size of these cations along the symmetry axis is much the same as along any direction perpendicular to the symmetry axis. The Mössbauer spectra for $\text{Fe}_2\text{Mn}_2\text{Cu}_3$ 1 and $\text{Fe}_2\text{Co}_2\text{Cu}_3$ 2 suggest that the $[\text{Fe}(\text{C}_5\text{Me}_5)_2]^+$ units occupy two sites with a 50/50 distribution. We may then assume that the five-fold symmetry axis

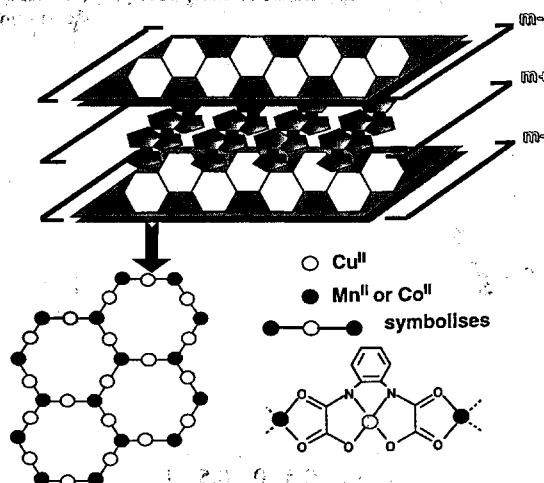


Fig. 7 Schematic representation of the $[\text{M}'(\text{C}_5\text{Me}_5)_2]_2\text{M}_2[\text{Cu}(\text{opba})]_3\cdot(\text{DMSO})_x\cdot(\text{H}_2\text{O})_y$ compounds (see text)

of $[\text{Fe}(\text{C}_5\text{Me}_5)_2]^+$ units is perpendicular to the layers for one of the sites and parallel for the other site. Alternatively, all the five-fold symmetry axes might be parallel to each other with, however, different positions of the $[\text{Fe}(\text{C}_5\text{Me}_5)_2]^+$ units with respect to the honeycomb planes. Such a situation is visualized in Fig. 7. In the absence of additional structural information, we cannot go further in this discussion. We can mention here that other layered compounds in which metallocenium cations are intercalated between the layers have been described.^{23–28}

Let us now focus on the magnetic properties of our compounds. All four present the typical features of ferrimagnets exhibiting spontaneous magnetization below a critical temperature T_C . What immediately emerges from our magnetic data is that the nature of the decamethylmetallocenium cation plays a minor role in the magnetic properties, except in enhancing the number of spins and saturation magnetization, and providing an internal field to affect the shape of the magnetic hysteresis loops. The two compounds with the $\text{Mn}_2[\text{Cu}(\text{opba})]_3$ skeleton order around 14 K; the other two compounds with the $\text{Co}_2[\text{Cu}(\text{opba})]_3$ skeleton order around 27 K. The $[\text{Fe}(\text{C}_5\text{Me}_5)_2]^+$ cations in $\text{Fe}_2\text{Mn}_2\text{Cu}_3$ **1** and $\text{Fe}_2\text{Co}_2\text{Cu}_3$ **2** essentially behave as simple paramagnetic ions embedded in a two-dimensional ferrimagnetic network.

As already observed,²⁹ the long-range magnetic ordering temperature, T_C , is higher for the $\text{Co}_2[\text{Cu}(\text{opba})]_3$ than for the $\text{Mn}_2[\text{Cu}(\text{opba})]_3$ compounds. Furthermore, the coercivity is remarkably strong in the former case, and negligibly weak in the latter. $\text{Co}_2\text{Co}_2\text{Cu}_3$ **4** exhibits one of the largest coercive fields (5.3×10^3 Oe) reported so far for a molecular-based magnet. The value of the coercive field at a given temperature for a polycrystalline magnet depends on both the chemical nature of the compound and some structural factors such as the size and the shape of the grains within the sample. Concerning the chemical nature of the compound, the key role is played by the magnetic anisotropy of the spin carriers which prevents the domains from rotating freely when applying the field. In the present case, the large coercivity arises from the strong orbital contribution of the Co^{II} ion in octahedral surroundings within the layer.²⁹

It is interesting to note that, in spite of its strong magnetic anisotropy, the $[\text{Fe}(\text{C}_5\text{Me}_5)_2]^+$ cation does not increase the coercivity of $\text{Fe}_2\text{Co}_2\text{Cu}_3$ **2** with respect to that of $\text{Co}_2\text{Co}_2\text{Cu}_3$ **4**. On the contrary, $[\text{Fe}(\text{C}_5\text{Me}_5)_2]^+$ seems to exert a counter-effect. As a matter of fact, the coercive fields in the same conditions are 3.5×10^4 Oe for $\text{Fe}_2\text{Co}_2\text{Cu}_3$ **2** and 5.3×10^3 Oe for $\text{Co}_2\text{Co}_2\text{Cu}_3$ **4**.

The two main pieces of information arising from this work are the following: (i) the two-dimensional ferrimagnets with the $\text{Co}_2[\text{Cu}(\text{opba})]_3$ motif may exhibit exceptionally strong coercivities; (ii) it is probably not possible to tune the magnetic properties of the $\text{cat}_2\text{M}_2[\text{Cu}(\text{opba})]_3 \cdot \text{S}$ compounds through the nature of the cat^+ cation. In particular, using a cat^+ paramagnetic cation does not result in an increase of the critical temperature.

References

- 1 J. S. Miller, J. C. Calabrese, A. J. Epstein, R. W. Bigelow, J. H. Zang and W. M. Reiff, *J. Chem. Soc., Chem. Commun.*, 1986, 1026.
- 2 Y. Pei, M. Verdaguer, O. Kahn, J. Sletten and J. P. Renard, *J. Am. Chem. Soc.*, 1986, **108**, 428.
- 3 J. S. Miller, J. C. Calabrese, H. Rommelman, S. R. Chittipedi, J. H. Zang, W. M. Reiff and A. J. Epstein, *J. Am. Chem. Soc.*, 1987, **109**, 769.
- 4 O. Kahn, Y. Pei, M. Verdaguer, J. P. Renard and J. Sletten, *J. Am. Chem. Soc.*, 1988, **110**, 782.
- 5 K. Nakatani, P. Bergerat, E. Codjovi, C. Mathonière, Y. Pei and O. Kahn, *Inorg. Chem.*, 1991, **30**, 3977.
- 6 J. S. Miller, J. C. Calabrese, D. A. Dixon, A. J. Epstein, R. W. Bigelow, J. H. Zhang and W. M. Reiff, *J. Am. Chem. Soc.*, 1987, **109**, 769.
- 7 W. E. Broderick, J. A. Thompson, E. P. Day and B. M. Hoffman, *Science*, 1990, **249**, 410.
- 8 G. T. Yee, J. M. Manriquez, D. A. Dixon, R. S. McLean, D. M. Groski, R. B. Flippen, K. S. Narayan, A. J. Epstein and J. S. Miller, *Adv. Mater.*, 1991, **3**, 309.
- 9 W. E. Broderick and B. M. Hoffman, *J. Am. Chem. Soc.*, 1991, **113**, 6334.
- 10 D. M. Eichhorn, D. C. Skee, W. E. Broderick and B. M. Hoffman, *Inorg. Chem.*, 1993, **32**, 491.
- 11 J. S. Miller and A. J. Epstein, *Angew. Chem., Int. Ed. Engl.*, 1994, **33**, 385.
- 12 O. Kahn, *Adv. Inorg. Chem.*, 1995, **43**, 179.
- 13 K. Nakatani, J. Y. Carriat, Y. Journaux, O. Kahn, F. Lioet, J. P. Renard, Y. Pei, J. Sletten and M. Vergaguer, *J. Am. Chem. Soc.*, 1989, **111**, 5739.
- 14 F. Lioet, M. Julve, R. Ruiz, Y. Journaux, K. Nakatani, O. Kahn and J. Sletten, *Inorg. Chem.*, 1993, **32**, 27.
- 15 H. O. Stumpf, Y. Pei, O. Kahn, J. Sletten and J. P. Renard, *J. Am. Chem. Soc.*, 1993, **115**, 6738.
- 16 H. O. Stumpf, L. Ouahab, Y. Pei, D. Grandjean and O. Kahn, *Science*, 1993, **261**, 447.
- 17 H. O. Stumpf, L. Ouahab, Y. Pei, P. Bergerat, O. Kahn, *J. Am. Chem. Soc.*, 1994, **116**, 3866.
- 18 O. Kahn, *Molecular Magnetism*, VCH, New York, 1993.
- 19 J. S. Miller and A. J. Epstein, *Angew. Chem., Int. Ed. Engl.*, 1994, **33**, 385.
- 20 S. Turner, C. Michaut, O. Kahn, L. Ouahab, A. Lecas and E. Amouyal, *New J. Chem.*, 1995, **19**, 773.
- 21 F. Palacio, F. J. Lazaro and A. J. van Duyneveldt, *Mol. Cryst. Liq. Cryst.*, 1989, **176**, 289.
- 22 G. K. Wertheim and R. H. Herber, Jr., *J. Chem. Phys.*, 1963, **38**, 2106.
- 23 R. Clement, W. B. Davles, K. A. Ford, M. L. H. Green and A. J. Jacobson, *Inorg. Chem.*, 1978, **17**, 2754.
- 24 R. Clement and M. L. H. Green, *J. Chem. Soc., Dalton Trans.*, 1979, **10**, 1566.
- 25 J. P. Audière, R. Clement, F. Mathey and C. Mazières, *Physica B*, 1980, **99**, 133.
- 26 R. Clement, *J. Chem. Soc., Chem. Commun.*, 1980, 647.
- 27 Y. Mathey, R. Clement, C. Sourisseau and G. Lucazeau, *Inorg. Chem.*, 1980, **19**, 2773.
- 28 R. Clement, *J. Am. Chem. Soc.*, 1981, **103**, 6998.
- 29 H. O. Stumpf, Y. Pei, C. Michaut, O. Kahn, J. P. Renard and L. Ouahab, *Chem. Mater.*, 1994, **6**, 657.

Paper 6/02426B; Received 9th April, 1996